Synthesis and Crystal Structure of the Novel Dianion $[Re(CO)_3(\eta^5\text{-}7\text{-}CB_{10}H_{11})]^{2-}$. Reactions with Platina- and Palladaphosphine Chlorides†

Ian Blandford,‡ John C. Jeffery,‡ Paul A. Jelliss,§ and F. Gordon A. Stone*,§

Department of Chemistry, Baylor University, Waco, Texas 76798-7348, and the School of Chemistry, The University, Bristol BS8 1TS, U.K.

Received October 20, 1997

The salts $[X]_2[Re(CO)_3(\eta^5\text{-}7\text{-}CB_{10}H_{11})]$ (X = $N(PPh_3)_2$ (**2a**), X = $NEt_3(CH_2Ph)$ (**2b**)) have been synthesized from the reaction between $[Na]_3[nido\text{-}7\text{-}CB_{10}H_{11}]$ and $[ReBr(THF)_2(CO)_3]$ (THF = tetrahydrofuran) followed by addition of XCl. An X-ray diffraction study revealed that **2b** crystallizes in the orthorhombic space group $Pna2_1$. The anion of **2a** could not be oxidized by a host of oxidants with the exception of I_2, which yielded the salt $[N(PPh_3)_2][ReI(CO)_3(\eta^5\text{-}7\text{-}CB_{10}H_{11})]$ (**3**). The neutral bimetallic complexes $[RePt(CO)_3(L)_2(\eta^5\text{-}7\text{-}CB_{10}H_{11})]$ (L = PPh_3 (**4a**), L = PEt_3 (**4b**), $(L)_2 = Ph_2P(CH_2)_2PPh_2$ (**4c**)) have been prepared by treating **2a** in THF with $[PtCl_2(L)_2]$ in the presence of $TlPF_6$. X-ray diffraction revealed that compound **4a** crystallizes in the monoclinic space group $C2/c$. The molecule contains a bridging *nido*-7-$CB_{10}H_{11}$ ligand which is η^5-coordinated to the Re atom and is bound to the Pt atom by a B_β-H⇀Pt agostic bond. The compound $[RePd(CO)_3\{Ph_2P(CH_2)_2PPh_2\}(\eta^5\text{-}7\text{-}CB_{10}H_{11})]$ (**5a**) has been prepared by treating **2a** with $[PdCl_2\{Ph_2P(CH_2)_2PPh_2\}]$ in THF in the presence of $TlPF_6$. X-ray diffraction showed that **5a** crystallizes in the orthorhombic space group $P2_12_12_1$, and the structure in the solid-state is similar to that of **4a** but with a B_β-H⇀Pd agostic bond. In solution, an exchange occurs on the NMR time scale between the B−H bonds in the coordinating CBBBB face which form the B−H⇀Pd linkage, thus generating a pseudo plane of symmetry in the molecule. Treatment of CH_2Cl_2 solutions of **5a** with CNR (R = Bu^t, $C_6H_3Me_2$-2,6) at −78 °C yields the complexes $[RePd(CO)_2(CNR)\{Ph_2P(CH_2)_2PPh_2\}(\eta^5\text{-}7\text{-}CB_{10}H_{11})]$ (R = Bu^t (**5b**), R = $C_6H_3Me_2$-2,6 (**5c**)). The IR and NMR spectra of the new compounds are discussed.

Introduction

The first rhenacarborane $[Cs][Re(CO)_3(\eta^5\text{-}7,8\text{-}C_2B_9H_{11})]$ (**1**) was reported over 30 years ago by Hawthorne et al.[1] This salt was synthesized by treatment of $[ReBr(CO)_5]$ with $[Na]_2[nido\text{-}7,8\text{-}C_2B_9H_{11}]$ in refluxing THF, followed by addition of CsCl. The structure of **1** was verified by an X-ray crystal structure determination,[2] Chart 1. To date there have been few advances in rhenacarborane chemistry; what little study that has been carried out is based on the syntheses of the anions $[Re(CO)_3(\eta^5\text{-}7,8\text{-}R_2\text{-}7,8\text{-}C_2B_9H_9)]$ (R = H, alkyl, aryl) which are directly related to **1**.[3] Indeed, research undertaken in our laboratory to investigate the reactivity of **1** yielded negative results with no apparent reaction occurring with H^+ or $[Au(PPh_3)]^+$ to give Re−H or Re−Au bonds, respectively.[4]

We have recently found the synthon $[nido\text{-}7\text{-}CB_{10}H_{11}]^{3-}$ increasingly useful in our quest for novel metallacarboranes,[5] and we now report its use in the unexplored arena of rhena−monocarbon−carborane chemistry.

Results and Discussion

Using a carefully orchestrated procedure, both $[Na]_3[nido\text{-}7\text{-}CB_{10}H_{11}]$ and $[ReBr(THF)_2(CO)_3]$ are generated in refluxing THF solutions, which are then combined at ca. 60 °C. Workup following addition of $[N(PPh_3)_2]Cl$ or $[NEt_3(CH_2Ph)]Cl$, respectively, gives the new salts $[X]_2[Re(CO)_3(\eta^5\text{-}7\text{-}CB_{10}H_{11})]$ (X = $N(PPh_3)_2$ (**2a**), X = $NEt_3(CH_2Ph)$ (**2b**)) (Table 1). The IR spectrum of **2a** in CH_2Cl_2 displays ν_{max}(CO) absorptions at 1964 (s) and 1854 (s br) cm^{-1} and these may be compared with those of **1** measured in THF at 2002 (vs), 1903 (vs), and 1894 (vs) cm^{-1} (**1** is almost completely insoluble in CH_2Cl_2,

† The compounds described in this paper have a rhenium atom incorporated into a *closo*-1-carba-2-rhenadodecaborane structure. However, to avoid a complicated nomenclature for the complexes reported and to relate them to the many known rhenium species with η^5-coordinated cyclopentadienyl ligands, we treat the cages as *nido*-11-vertex ligands with numbering as for an icosahedron from which the twelfth vertex has been removed.

‡ University of Bristol.

§ Baylor University.

(1) Hawthorne, M. F.; Andrews, T. D. *J. Am. Chem. Soc.* **1965**, *87*, 2496; *Ibid.* **1968**, *90*, 879.

(2) Zalkin, A.; Hopkins, T. E.; Templeton, D. H. *Inorg. Chem.* **1966**, *5*, 1189.

(3) (a) Zakharkin, L. I.; Ol'shevskaya, V. A. *Izv. Akad. Nauk SSSR, Ser. Khim.* **1987**, 2296. (b) Zakharkin, L. I.; Ol'shevskaya, V. A.; Poroshina, T.-Yu. *Metallorg. Khim.* **1989**, *2*, 363. (c) Chetcuti, P. A.; Moser, P.; Rihs, G. *Organometallics* **1991**, *10*, 2895. (d) Grimes, R. N. In *Comprehensive Organometallic Chemistry II*; Abel, E. W., Stone, F. G. A., Wilkinson, G., Eds.; Elsevier Science Ltd.: Oxford, 1995; Vol. 1, Section 9.

(4) Li, S. Unpublished results.

(5) Batten, S. A.; Jeffery, J. C.; Jones, P. L.; Mullica, D. F.; Rudd, M. D.; Sappenfield, E. L.; Stone, F. G. A.; Wolf, A. *Inorg. Chem.* **1997**, *36*, 2570.

S0276-7333(97)00914-X CCC: $15.00
Publication on Web 03/04/1998

Table 1. Analytical and Physical Data

compd	color	yield (%)	ν_{max}(CO)[a] (cm^{-1})	anal. (%)[b] C	H
2a, $[N(PPh_3)_2][Re(CO)_3(\eta^5\text{-}7\text{-}CB_{10}H_{11})]$	pale yellow	91	1964 (s), 1854 (s br)	61.9 (61.7)	4.7 (4.8)[c]
3, $[N(PPh_3)_2][ReI(CO)_3(\eta^5\text{-}7\text{-}CB_{10}H_{11})]$	bright yellow	80	2078 (s), 2020 (s), 1988 (m)	44.5 (45.0)	3.2 (3.9)[d]
4a, $[RePt(CO)_3(PPh_3)_2(\eta^5\text{-}7\text{-}CB_{10}H_{11})]$	yellow	92	2030 (vs), 1964 (m), 1932 (s)	41.7 (42.8)	3.6 (3.7)
4b, $[RePt(CO)_3(PEt_3)_2(\eta^5\text{-}7\text{-}CB_{10}H_{11})]$	yellow	91	2022 (vs), 1954 (m), 1924 (s)	22.5 (23.1)	4.8 (5.0)
4c, $[RePt(CO)_3\{Ph_2P(CH_2)_2PPh_2\}(\eta^5\text{-}7\text{-}CB_{10}H_{11})]$	yellow	85	2030 (vs), 1964 (m), 1934 (s)	34.8 (34.5)	3.5 (3.5)
5a, $[RePd(CO)_3\{Ph_2P(CH_2)_2PPh_2\}(\eta^5\text{-}7\text{-}CB_{10}H_{11})]$	orange	78	2024 (vs), 1956 (m), 1926 (s)	39.9 (39.8)	3.9 (3.9)
5b, $[RePd(CO)_2(CNBu^t)\{Ph_2P(CH_2)_2PPh_2\}(\eta^5\text{-}7\text{-}CB_{10}H_{11})]$	orange	53	1955 (m), 1898 (s)[e]	42.5 (42.5)	4.6 (4.6)[f]
5c, $[RePd(CO)_2(CNC_6H_3Me_2\text{-}2,6)\{Ph_2P(CH_2)_2PPh_2\}(\eta^5\text{-}7\text{-}CB_{10}H_{11})]$	orange-brown	67	1951 (m), 1900 (s)[g]	45.2 (45.3)	4.4 (4.4)[h]

[a] Measured in CH_2Cl_2; medium-intensity broad bands observed at ca. 2550 cm^{-1} in the spectra of all of the compounds are due to B−H absorptions. [b] Calculated values are given in parentheses. [c] N, 1.8 (1.9). [d] N, 1.0 (1.3). [e] ν_{max}(NC) 2149 (m br) cm^{-1}. [f] N, 1.5 (1.5). [g] ν_{max}(NC) 2121 (m br) cm^{-1}. [h] N, 1.4 (1.4).

Chart 1

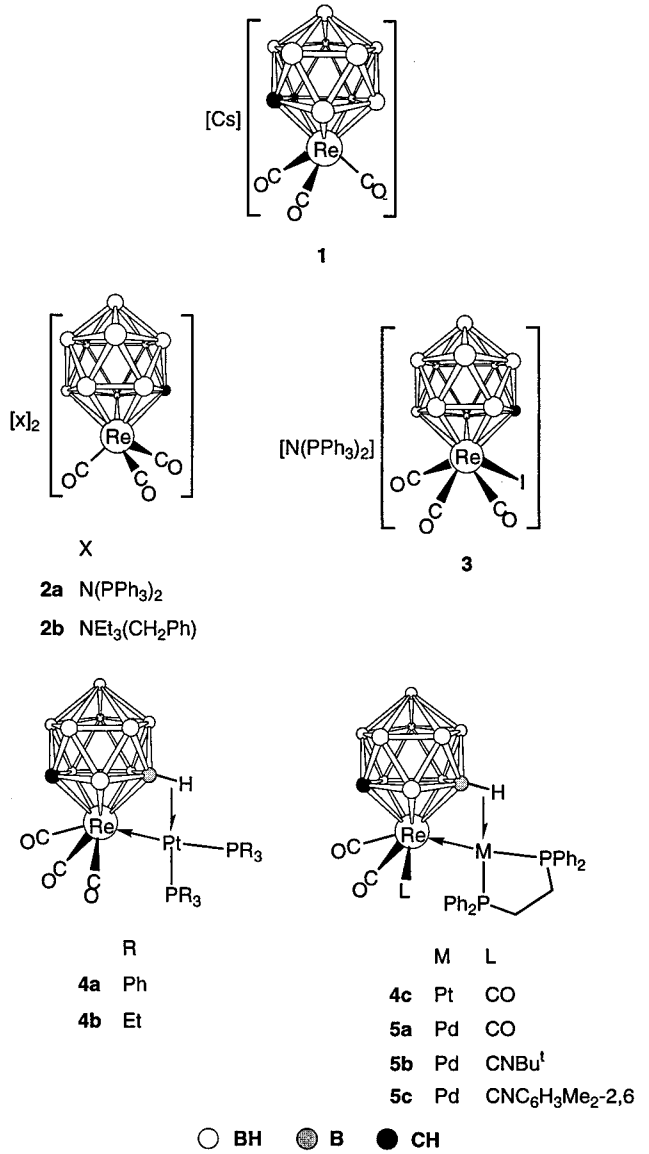

while **2a** has very low solubility in THF). The appearance of absorptions toward lower frequency in **2a** may be attributed to the additional negative charge carried by the monocarbollide complex compared to the uninegative anion in **1**. The NMR spectra of **2a** (Tables 2 and 3) are relatively simple, with the ^1H NMR spectrum revealing a broad signal at δ 1.50 due to the cage CH protons and the $^{13}C\{^1H\}$ NMR spectrum showing a broad resonance due to the cage carbon nucleus at δ 31.8. The latter spectrum also clearly shows a single peak arising from the carbonyl carbon nuclei at δ 205.8, which implies that the $Re(CO)_3$ unit is "spinning" relative to the cage about an axis through the Re and the centroid of the ligating CBBBB ring, i.e., there is local C_{3v} symmetry at the Re atom in solution. A similar process must be occurring in **1**, which also displays a single peak due to the carbonyl carbon nuclei in the $^{13}C\{^1H\}$ NMR spectrum at δ 199.0 (acetone-d_6). A $^{13}C\{^1H\}$ NMR spectrum of **2a** measured at −90 °C showed that the single CO resonance was maintained, and so the spinning could not be frozen out. The $^{11}B\{^1H\}$ NMR spectrum of **2a** reflects the permanent cage C_s symmetry with five peaks having peak integral ratios of 1:3:2:2:2, the second signal being due to fortuitous overlap of two resonances.

To compare the structure of the new dianion $[Re(CO)_3(\eta^5\text{-}7\text{-}CB_{10}H_{11})]^{2-}$ with that of the monoanion of **1**, single crystals of the $[NEt_3(CH_2Ph)]^+$ salt **2b** were grown and analyzed by X-ray diffraction. The structure determination was also necessary as a starting point for simple molecular orbital calculations. The structure is shown in Figure 1, and significant bond lengths and angles are given in Table 4. It is immediately apparent that the binding of the $Re(CO)_3$ unit in **2b** (Re−C(1) 2.322(4) Å, Re−B(2) 2.327(5) Å, Re−B(3) 2.364(4) Å, Re−B(4) 2.362(4) Å, Re−B(5) 2.313(5) Å) is very similar to that in **1** (Re−C 2.31 and 2.31 Å, Re−B 2.32, 2.35, and 2.35 Å).[2] All Re−C−O bonds in **2b** are near-linear (average 177.4°) as was observed in compound **1** (average 176.3°).

It was mentioned previously that compound **1** has so far proven to be unreactive toward electrophilic centers such as H^+ and $[Au(PPh_3)]^+$, and we believe that this may be due to the burying of the negative charge within the *closo*-3,1,2-ReC_2B_9 cage framework leading to low nucleophilicity and low basicity at the metal center. Our hope was that with an additional negative charge associated with the *closo*-2,1-$ReCB_{10}$ cage, complex **2a** might be a more potent reactant. Initial reactivity studies were centered on attempting to protonate or oxidize **2a** directly. However, the complex displayed no propensity to form a hydrido species $[ReH(CO)_3(\eta^5\text{-}7\text{-}CB_{10}H_{11})]^-$ upon addition of H^+ derived from a variety of sources ($HBF_4{\cdot}OEt_2$, $HCl(Et_2O)$, CF_3CO_2H). Furthermore, **2a** showed no ability to form stable complexes of the type $[ReL(CO)_3(\eta^5\text{-}7\text{-}CB_{10}H_{11})]$ upon treatment with several oxidants in the presence of ligands L (Scheme 1). The lack of formation of tractable products, in particular $[Re(THF)(CO)_3(\eta^5\text{-}7\text{-}CB_{10}H_{11})]$, was disappointing as a related dicarbollide species $[Ru(THF)(CO)_2(\eta^5\text{-}7,8\text{-}R_2\text{-}7,8\text{-}C_2B_9H_9)]$ (R = H, Me) has shown

Table 2. ^{1}H and ^{13}C NMR Data[a]

compd	1H (δ)[b]	^{13}C (δ)[c]
2a	1.50 (s br, 1 H, CH), 7.46−7.67 (m, 60 H, Ph)	205.8 (CO), 134.0−126.7 (Ph), 31.8 (br, CH)
3	2.94 (s br, 1 H, CH), 7.48−7.67 (m, 30 H, Ph)	200.3 (CO × 1), 188.4 (CO × 2), 134.1−126.8 (Ph), 60.8 (br, CH)
4a	−6.78 (m br, 1 H, B−H⇀Pt, *J*(PtH) ca. 460), 2.30 (s br, 1 H, CH), 6.59−7.94 (m, 30 H, Ph)	197.2, 196.1, 194.6 (CO), 135.4−128.8 (Ph), 40.9 (br, CH)
4b	−7.52 (m br, 1 H, B−H⇀Pt, *J*(PtH) ca. 470), 1.10, 1.22 (m × 2, 18 H, Me), 2.18, 2.32 (m × 2, 12 H, CH_2)	197.7 (CO × 1), 194.9 (br, CO × 2), 41.2 (br, CH), 20.7, 19.4 (m × 2, CH_2), 9.2, 8.6 (m × 2, Me)
4c	−4.85 (m br, 1 H, B−H⇀Pt, *J*(PtH) 585), 2.01 (m br, 1 H, CH_2), 2.19 (s br, 1 H, CH), 2.65 (m br, 3 H, CH_2), 7.50−7.82 (m, 20 H, Ph)	196.3 (br, CO), 135.4−129.4 (Ph), 40.6 (br, CH), 31.8, 23.8 (m br × 2, CH_2)[d]
5a	2.25 (s br, 1 H, CH), 2.35, 2.76 (m × 2, 4 H, CH_2), 7.49−7.75 (m, 20 H, Ph)	196.9 (CO × 1), 194.0 (CO × 2), 134.2−126.4 (Ph), 41.2 (br, CH), 32.1 (dd, CH_2, *J*(PC) 36, 20), 23.8 (dd, CH_2, *J*(PC) 33, 12)
5b	1.36 (s, 9 H, CMe_3), 2.17 (s br, 1 H, CH), 2.18, 2.26, 2.68, 2.77 (m × 4, 4H, CH_2), 7.47−7.74 (m, 20 H, Ph)	197.9, 197.8 (CO), 178.8 (CN), 134.2−127.8 (Ph), 58.4 (CMe_3), 41.1 (br, CH), 32.4 (dd, CH_2, *J*(PC) 55, 21), 30.9 (CMe_3), 23.2 (dd, CH_2, *J*(PC) 30, 11)
5c[e]	2.52, 2.59 (m × 2, 2 H, CH_2), 2.76 (s br, 1 H, CH), 2.79, 2.82 (s × 2, 6 H, $C_6H_3Me_2$-2,6), 3.11, 3.21 (m × 2, 2 H, CH_2), 7.12−7.90 (m, 23 H, Ph and $C_6H_3Me_2$-2,6)	197.9 (CO), 135.3−128.4 (Ph and $C_6H_3Me_2$-2,6), 41.2 (br, CH), 19.0, 18.9 ($C_6H_3Me_2$-2,6)[d]

[a] Chemical shifts (δ) are given in ppm, coupling constants (*J*) in hertz; measurements performed at room temperature in CD_2Cl_2, unless otherwise stated. [b] Resonances for terminal BH protons occur as broad unresolved signals in the range δ ca. −2 to 3. [c] ^{1}H-decoupled chemical shifts are positive to higher frequency of $SiMe_4$. [d] Some peaks are not observed due to the low solubility of the complex. [e] Measured in acetone-d_6.

Table 3. ^{11}B and ^{31}P NMR Data[a]

compd	^{11}B (δ)[b]	^{31}P (δ)[c]
2a	−4.6 (1 B), −11.1 (3 B), −15.1 (2 B), −18.5 (2 B), −21.4 (2 B)	
3	11.2 (1 B), −4.7 (3 B), −5.4 (2 B), −11.5 (2 B), −15.6 (2 B)	
4a	28.7 (1 B, B−H⇀Pt), 0.8 (1 B), −5.4 (2 B), −9.6 (1 B), −13.0 (1 B), −15.1 (3 B), −18.4 (1 B)	19.4 (d br, *J*(PP) 20, *J*(PtP) 3696), 12.7 (d, *J*(PP) 20, *J*(PtP) 2927)
4b	25.3 (1 B, B−H⇀Pt), 0.9 (1 B), −5.7 (2 B), −9.9 (1 B), −13.1 (1 B), −15.0 (2 B), −16.1 (1 B), −18.4 (1 B)	16.6 (d, *J*(PP) 15, *J*(PtP) 2789), 9.4 (d br, *J*(PP) 15, *J*(PtP) 3415)
4c	26.2 (1 B, B−H⇀Pt), 1.1 (1 B), −5.3 (2 B), −10.3 (1 B), −12.9 (1 B), −15.6 (2 B), −17.3 (1 B), −18.2 (1 B)	58.2 (d, *J*(PP) 6, *J*(PtP) 2831), 53.1 (d br, *J*(PP) 6, *J*(PtP) 3374)
5a	0.4 (2 B), −8.5 (4 B), −13.8 (2 B), −17.7 (2 B)	62.9, 61.0 (AB, *J*(AB) 23)
5b	9.3 (1 B), −2.1 (1 B), −9.0 (1 B), −10.4 (3 B), −12.9 (2 B), −18.0 (2 B)	58.2, 50.5 (d × 2, *J*(PP) 35)
5c[d]	−1.6, −8.9, −9.7, −13.1, −17.9[e]	61.4, 57.6 (AB, *J*(AB) 31)

[a] Chemical shifts (δ) are given in ppm, coupling constants (*J*) in hertz; measurements performed at room temperature in CD_2Cl_2, unless otherwise stated. [b] ^{1}H-decoupled chemical shifts are positive to higher frequency of $BF_3{\cdot}OEt_2$ (external). The B−H⇀Pt assignments were made from fully coupled ^{11}B spectra. [c] ^{1}H-decoupled chemical shifts are positive to higher frequency of 85% H_3PO_4 (external). [d] Measured in acetone-d_6. [e] Peak integrals could not be confidently assigned due to the extremely weak spectrum, a result of the very low solubility of the product.

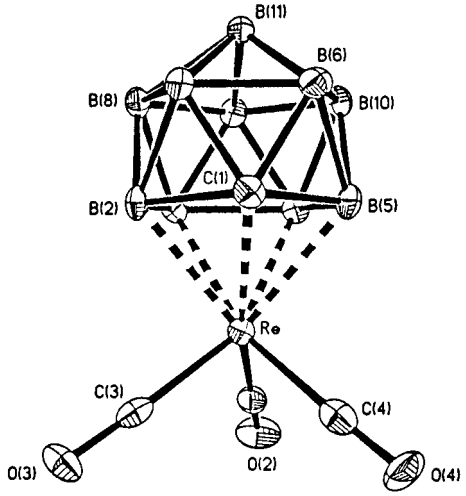

Figure 1. Structure of the anion of $[NEt_3(CH_2Ph)]_2[Re(CO)_3(\eta^5\text{-}7\text{-}CB_{10}H_{11})]$ (**2b**), showing the crystallographic labeling scheme. Thermal ellipsoids are shown at the 40% probability level. Hydrogen atoms are omitted for clarity.

high reactivity and yielded a fascinating array of new mono- and bimetallic complexes.[6]

There was one exception to the failure of attempts to oxidize complex **2a**. Low-temperature treatment with just under 1 equiv of I_2 gave a new rhenacarborane−iodo complex $[N(PPh_3)_2][ReI(CO)_3(\eta^5\text{-}7\text{-}CB_{10}H_{11})]$ (**3**) in good yield. It is particularly important not to add too much I_2 in this reaction as the carborane cage is itself susceptible to attack by the halogen. The IR spectrum of compound **3** shows the expected pattern of ν_{max}(CO) absorption bands at 2078 (s), 2020 (s), and 1988 (m) cm^{-1} (Table 1). The NMR data (Tables 2 and 3) are consistent with a C_s structure in solution with a plane of symmetry encompassing the Re, cage C, and I atoms and also a CO ligand transoid to the iodine. The $^{13}C\{^{1}H\}$ NMR spectrum of **3** reveals two carbonyl carbon resonances at δ 200.3 and 188.4 with a peak integral ratio of 1:2. The ^{1}H NMR spectrum shows a broad peak at δ 2.94 due to the cage CH proton, which is shifted considerably downfield of the corresponding signal for **2a**, presumably as a result of the increase in the oxidation state at the rhenium center. It was hoped that the new salt **3** would, in the presence of $TlPF_6$ or $AgBF_4$ and ligands L (L = donor solvents, phosphines, alkynes), also give complexes of the type $[ReL(CO)_3(\eta^5\text{-}7\text{-}CB_{10}H_{11})]$. Again, however, this strategy proved unsuccessful.

To understand more regarding the reactivity or rather lack of reactivity of **2a** at the rhenium center, a simple molecular orbital analysis was carried out.[7] To facilitate ZINDO and EHMO calculations, the Re atom was

(6) (a) Anderson, S.; Mullica, D. F.; Sappenfield, E. L.; Stone, F. G. A. *Organometallics* **1995**, *14*, 3516. (b) Anderson, S.; Mullica, D. F.; Sappenfield, E. L.; Stone, F. G. A. *Organometallics* **1996**, *15*, 1676. (c) Anderson, S.; Jeffery, J. C.; Liao, Y.-H.; Mullica, D. F.; Sappenfield, E. L.; Stone, F. G. A. *Organometallics* **1997**, *16*, 958. (d) Jeffery, J. C.; Jelliss, P. A.; Liao, Y.-H.; Stone, F. G. A. *J. Organomet. Chem.* **1997**, in press. (e) Jeffery, J. C.; Jelliss, P. A.; Psillakis, E.; Rudd, G. E. A.; Stone, F. G. A. *J. Organomet. Chem.* **1997**, in press.

Table 4. Selected Internuclear Distances (Å) and Angles (deg) for the Anion of $[NEt_3(CH_2Ph)]_2[Re(CO)_3(\eta^5\text{-}7\text{-}CB_{10}H_{11})]$ (2b) with ESD's in Parentheses

Re−C(3)	1.888(4)	Re−C(2)	1.896(4)	Re−C(4)	1.916(4)	Re−B(5)	2.313(5)
Re−C(1)	2.322(4)	Re−B(2)	2.327(5)	Re−B(4)	2.362(4)	Re−B(3)	2.364(4)
C(2)−O(2)	1.164(4)	C(3)−O(3)	1.188(4)	C(4)−O(4)	1.159(4)		

C(3)−Re−C(2)	93.5(2)	C(3)−Re−C(4)	90.0(2)	C(2)−Re−C(4)	89.6(2)
C(3)−Re−B(5)	146.3(2)	C(2)−Re−B(5)	120.0(2)	C(4)−Re−B(5)	87.3(2)
C(3)−Re−C(1)	103.67(14)	C(2)−Re−C(1)	160.8(2)	C(4)−Re−C(1)	98.7(2)
B(5)−Re−C(1)	43.92(14)	C(3)−Re−B(2)	82.8(2)	C(2)−Re−B(2)	132.5(2)
C(4)−Re−B(2)	137.4(2)	B(5)−Re−B(2)	76.7(2)	C(1)−Re−B(2)	43.98(13)
C(3)−Re−B(4)	151.75(14)	C(2)−Re−B(4)	86.06(14)	C(4)−Re−B(4)	118.3(2)
B(5)−Re−B(4)	45.5(2)	C(1)−Re−B(4)	74.79(13)	B(2)−Re−B(4)	76.9(2)
C(3)−Re−B(3)	106.6(2)	C(2)−Re−B(3)	92.9(2)	C(4)−Re−B(3)	163.0(2)
B(5)−Re−B(3)	76.85(14)	C(1)−Re−B(3)	74.22(14)	B(2)−Re−B(3)	44.7(2)
B(4)−Re−B(3)	45.35(14)	O(2)−C(2)−Re	177.0(3)	O(3)−C(3)−Re	177.3(3)
O(4)−C(4)−Re	177.9(4)				

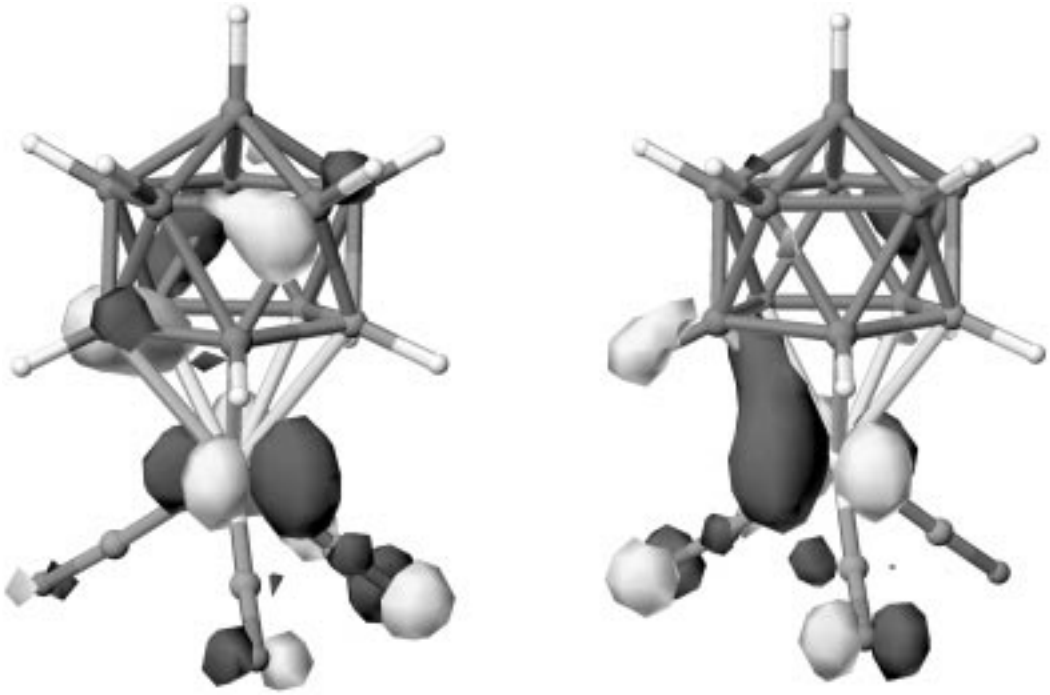

Figure 2. ZINDO-calculated HOMO (left) and HOMO-1 (right) frontier orbitals for the anion $[Tc(CO)_3(\eta^5\text{-}7\text{-}CB_{10}H_{11})]^{2-}$.

Scheme 1. Unsuccessful Attempts To Oxidize $[Re(CO)_3(\eta^5\text{-}7\text{-}CB_{10}H_{11})]^{2-}$

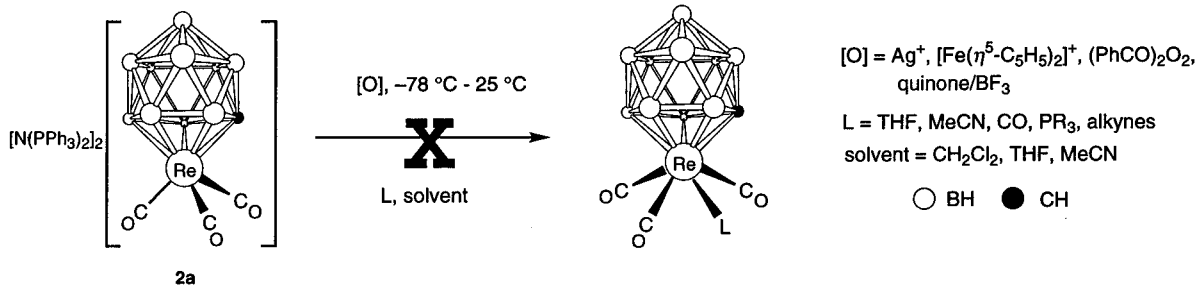

2a

replaced by Tc, an acceptable substitution on the basis of the homogeneity of the second and third row elements of transition metal group 7 elements in terms of chemistry and, especially, atomic radii.[8] Coordinates were taken directly from the X-ray structure determination of **2b**. The ZINDO calculation shows that although the frontier region HOMO (highest occupied molecular orbital) and HOMO-1 orbitals (Figure 2) are predominantly metal-based, there is some notable cage−ligand character. An EHMO calculation using conventional parameters gave a similar result. An EHMO frontier density calculation indicated that the negative charge was very diffuse and highly delocalized about the *closo*-2,1-$TcCB_{10}$ framework (and presumably the *closo*-2,1-$ReCB_{10}$ system also). This would seem to disfavor oxidation to give a stable species, as direct removal of polyhedral skeletal electrons from the metal−cage framework could easily lead to irreversible degra-

(7) *CaChe Scientific*; The Oxford Molecular Group: Oxford, U.K., 1994.

(8) Cotton, F. A.; Wilkinson, G. *Advanced Inorganic Chemistry*, 5th ed.; John Wiley and Sons: New York, 1988; Chapter 19-D.

dation. Indeed, cyclic voltammetry experiments run on CH_2Cl_2 solutions of **2a** indicate an irreversible 1 e^- oxidation is taking place at ca. −0.2 V, and this is accompanied by chemical decomposition of the compound. However, with such significant metal components in the HOMO and HOMO-1 orbitals, reaction of **2a** to give products with Re−M bonds may not necessarily be precluded. Therefore, an alternative approach to the employment of **2a** as a synthon would be to treat it with transition metal halide complexes.

A host of bimetallic rhenium−platinum complexes have been synthesized, with much interest focusing on their potential catalytic behavior.[9] It, therefore, seemed sensible to pursue a line of research into Re−M bond-forming reactions with a view to preparing novel rhenacarborane−platinum complexes. Reactions of **2a** with the compounds $[PtCl_2(L)_2]$ (L = PPh_3 or PEt_3, $(L)_2$ = $Ph_2P(CH_2)_2PPh_2$) in THF in the presence of $TlPF_6$ afforded the neutral complexes $[RePt(CO)_3(L)_2(\eta^5\text{-}7\text{-}CB_{10}H_{11})]$ (L = PPh_3 (**4a**), L = PEt_3 (**4b**), $(L)_2$ = $Ph_2P(CH_2)_2PPh_2$ (**4c**)). The new complexes were all formed in excellent yields and displayed almost identical IR spectra (Table 1), e.g., that of **4a** shows three ν_{max}(CO) absorptions at 2030 (vs), 1964 (m), and 1932 (s) cm^{-1}. The $^{11}B\{^1H\}$ and $^{31}P\{^1H\}$ NMR spectra (Table 3) of the complexes **4** indicated that they contained no symmetry elements. For instance, the $^{11}B\{^1H\}$ NMR spectrum of **4a** showed seven signals (1:1:2:1:1:3:1) with that at δ 28.7 diagnostic of the *B*−H⇀Pt boron nucleus, as determined by running a fully coupled ^{11}B NMR spectrum.[10] Indeed, for all of complexes **4**, when comparing the ^{11}B NMR with the $^{11}B\{^1H\}$ NMR spectra, it could be seen that the diagnostic low-field peak for the three-center two-electron B−H⇀Pt bond broadened slightly but no $^1H-^{11}B$ coupling could be resolved. This coupling would normally be expected to lie in the range 60−90 Hz, but as terminal B−H bonds show $^1H-^{11}B$ coupling which is invariably >100 Hz, there was little doubt as to the assignment of these peaks. The $^{31}P\{^1H\}$ NMR spectrum of **4a** confirmed the presence of two inequivalent PPh_3 ligands with doublet resonances at δ 19.4 (d br, *J*(PP) 20, *J*(PtP) 3696) and 12.7 (d, *J*(PP) 20, *J*(PtP) 2927 Hz). The broadness of the former peak indicates that this PPh_3 ligand lies trans to the B−H⇀Pt agostic group, with the quadrupolar boron nuclei exerting their customary influence. The $^{195}Pt-^{31}P$ satellite couplings are also typical for a 16 e^- square-planar platinum system in a metallacarborane complex.[11] The ^1H NMR spectra are also informative (Table 2), those for **4a**−**c** showing broad peaks in the range δ −4.85 to −7.52 due to the agostic B−*H*⇀Pt protons, although again no $^{11}B-^1H$ coupling could be resolved. The $^{13}C\{^1H\}$ NMR spectrum of **4a** showed resonances due to the three inequivalent CO carbon nuclei (δ 197.2, 196.1, and 194.6), reflecting the complete lack of symmetry in the molecule. The NMR measurements cannot differentiate between the two possible B−H⇀Pt agostic systems: a B_α−H⇀Pt bridge linkage, where a B−H bond adjacent (α) to the C−H vertex in the C*B*BBB cage face is utilized, or a B_β−H⇀Pt three-center bond, where a nonadjacent (β) B−H bond in the CB*B*BB face is employed. Either of these would lead to asymmetric structures. To solve this problem, an X-ray diffraction study was carried out on a single crystal of **4a**. The structure is shown in Figure 3, and important molecular parameters are given in Table 5.

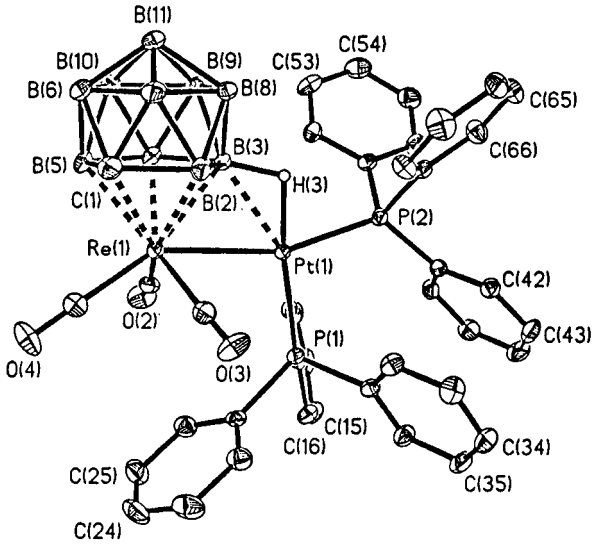

Figure 3. Structure of $[RePt(CO)_3(PPh_3)_2(\eta^5\text{-}7\text{-}CB_{10}H_{11})]$ (**4a**), showing the crystallographic labeling scheme. Thermal ellipsoids are shown at the 40% probability level. Only the agostic hydrogen atom is shown for clarity.

The Re(1)−Pt(1) bond (2.7931(4) Å) is marginally shorter than those found in the complexes $[RePtH_2(CO)_2(PPh_3)_2(\eta^5\text{-}C_5H_5)]$ (2.838(1) Å)[9c] and $[RePt(\mu\text{-}CO)\{\mu\text{-}Ph_2P(CH_2)PPh_2\}_2Cl_2(N_2C_6H_4Me\text{-}4)]$ (2.859(4) Å)[9d] and is spanned by the *nido*-7-$CB_{10}H_{11}$ ligand, which is in turn η^5-coordinated to the Re(1) atom (Re(1)−C(1) 2.315(3) Å, Re(1)−B(2) 2.336(3) Å, Re(1)−B(3) 2.254(4) Å, Re(1)−B(4) 2.340(4) Å, Re(1)−B(5) 2.307(3) Å). The Re(1)−B(3) bond is noticeably shorter than the remaining four Re−C/B contacts, due to the involvement of B(3) in the B(3)−H(3)⇀Pt(1) bridge. The agostic group gives rise to a close Pt(1)−B(3) contact (2.355(3) Å), and this is very similar to the *exo*-B−Pt bond length (2.313(8) Å) in a related complex $[MoPt(CO)_4(PPh_3)(\eta^6\text{-}7,9\text{-}Me_2\text{-}7,9\text{-}C_2B_{10}H_{10})]$.[11a] While the latter complex contains a very different carborane cage, there are structural similarities between the molybdenum−platinum species and complex **4a** with respect to the B−H⇀Pt(CO)(PPh_3) and $Mo(CO)_3$ fragments and the B−H⇀Pt(PPh_3)$_2$ and $Re(CO)_3$ groups of **4a**. The Re−C−O bond angles in **4a** are all close to linear with Re(1)−C(4)−O(4), which lies transoid to the Pt(PPh_3)$_2$ group, showing the least deviation (Re(1)−C(2)−O(2) 171.3(3)°, Re(1)−C(3)−O(3) 172.0(3)°, Re(1)−C(4)−O(4) 179.7(4)°). The other two carbonyl groups are tending toward an incipient bridging Re−C(O)···Pt arrangement, but the carbonyl carbons are not within bonding distance of the platinum (Pt(1)···C(2) 2.976 Å, Pt(1)···C(3) 2.957 Å). The Pt−P

(9) (a) Puddephatt, R. J.; Xiao, J. *Coord. Chem. Rev.* **1995**, *143*, 457 and references cited therein. (b) Bergamo, M.; Beringhelli, T.; Ciani, G.; D'Alfonso, G.; Moret, M.; Sironi, A. *Organometallics* **1996**, *15*, 1637 and references cited therein. (c) Casey, C. P.; Rutter, E. W., Jr.; Haller, K. J. *J. Am. Chem. Soc.* **1987**, *109*, 6886. (d) Carr, S. W.; Fontaine, X. L. R.; Shaw, B. L.; Thornton-Pett, M. *J. Chem. Soc., Dalton Trans.* **1988**, 769.

(10) (a) Stone, F. G. A. *Adv. Organomet. Chem.* **1990**, *31*, 53. (b) Brew, S. A.; Stone, F. G. A. *Adv. Organomet. Chem.* **1993**, *35*, 135. (c) Jelliss, P. A.; Stone, F. G. A. *J. Organomet. Chem.* **1995**, *500*, 307.

(11) (a) Dossett, S. J.; Mullica, D. F.; Sappenfield, E. L.; Stone, F. G. A.; Went, M. J. *J. Chem. Soc., Dalton Trans.* **1993**, 281. (b) Jeffery, J. C.; Jelliss, P. A.; Stone, F. G. A. *Inorg. Chem.* **1993**, *32*, 3943.

Table 5. Selected Internuclear Distances (Å) and Angles (deg) for $[RePt(CO)_3(PPh_3)_2(\eta^5\text{-}7\text{-}CB_{10}H_{11})]$ (4a) with ESD's in Parentheses

Pt(1)−P(1)	2.2950(8)	Pt(1)−P(2)	2.3137(8)	Pt(1)−B(3)	2.355(3)	Pt(1)−Re(1)	2.7931(4)
Pt(1)−H(3)	1.57(4)	Re(1)−C(2)	1.941(3)	Re(1)−C(3)	1.962(4)	Re(1)−C(4)	1.968(3)
Re(1)−B(3)	2.254(4)	Re(1)−B(5)	2.307(3)	Re(1)−C(1)	2.315(3)	Re(1)−B(2)	2.336(3)
Re(1)−B(4)	2.340(4)	B(3)−H(3)	1.37(4)	C(2)−O(2)	1.151(4)	C(4)−O(4)	1.143(4)
C(3)−O(3)	1.148(4)						

P(1)−Pt(1)−P(2)	96.51(3)	Pt(1)−Pt(1)−B(3)	154.45(9)	P(2)−Pt(1)−B(3)	109.03(9)
P(1)−Pt(1)−Re(1)	103.39(2)	P(2)−Pt(1)−Re(1)	160.10(2)	B(3)−Pt(1)−Re(1)	51.08(9)
C(2)−Re(1)−C(3)	110.23(13)	C(2)−Re(1)−C(4)	85.61(13)	C(3)−Re(1)−C(4)	84.56(14)
C(2)−Re(1)−Pt(1)	75.52(9)	C(3)−Re(1)−Pt(1)	74.62(9)	C(4)−Re(1)−Pt(1)	144.60(10)
B(9)−B(3)−Pt(1)	140.7(2)	B(8)−B(3)−Pt(1)	141.6(2)	B(4)−B(3)−Pt(1)	108.5(2)
B(2)−B(3)−Pt(1)	110.0(2)	Re(1)−B(3)−Pt(1)	74.56(11)	O(2)−C(2)−Re(1)	171.3(3)
O(4)−C(4)−Re(1)	179.7(4)	O(3)−C(3)−Re(1)	172.0(3)		

distances (average 2.304 Å) are very close to the average found for Pt−P bond lengths in four-coordinate platinum triphenylphosphine complexes (2.298 Å).[12] Most importantly, the X-ray structure of **4a** reveals that a B_β−H bond is used for agostic bonding. So few bimetallic complexes involving bridging *nido*-7-$CB_{10}H_{11}$ ligands have been synthesized and structurally characterized[5] that no pattern has been established as to which B−H site in the coordinating CBBBB face of the cage may be preferred for three-center two-electron bridge-bonding in such systems. There was no evidence in any of the complexes **4** of a second isomer with a B_α−H⇀Pt-bonded group. The remaining NMR spectral data for complexes **4a**−**c** are in accord with the structure established for **4a** by X-ray diffraction.

In light of success with the formation of compounds **4**, the study was extended to include palladium, particularly as organometallic complexes containing Re−Pd bonds are extremely rare.[13] Treatment of **2a** with $[PdCl_2\{Ph_2P(CH_2)_2PPh_2\}]$ in THF in the presence of $TlPF_6$ yielded the new complex $[RePd(CO)_3\{Ph_2P(CH_2)_2PPh_2\}(\eta^5\text{-}7\text{-}CB_{10}H_{11})]$ (**5a**). It was immediately obvious from NMR measurements at ambient temperatures that **5a** was somehow structurally different from **4c** in solution. However, a single-crystal X-ray diffraction study revealed a molecular structure very similar to that of **4a**. Before the anomalous NMR spectra are discussed, the results of this structure determination are presented. The molecule is shown in Figure 4, and selected bond lengths and angles are given in Table 6.

The salient structural features are similar to those of **4a**, with the Re−Pd bond (2.7858(4) Å) bridged by the *nido*-7-$CB_{10}H_{11}$ cage. Specifically, the B(4)−H(4) bond is used in the bridging B_β−H⇀Pd agostic system (Re−B(4) 2.272(4) Å, Pd−B(4) 2.333(4) Å). The Re−C−O bond angles are all close to linear (average 174.9°) with little or no tendency toward a semibridging Re−C(O)···Pd situation. The P(1)−Pd−P(2) angle of 85.22(4)° is understandably smaller than the P(1)−Pt(1)−P(2) angle (96.51(3)°) in **4a** because of the bite of the $Ph_2P(CH_2)_2PPh_2$ chelating ligand. The Pd−P bond lengths in **5a** (average 2.271 Å) are, as expected, fractionally less than the Pt−P lengths in **4a** (average 2.304 Å) but are close to the average (2.260 Å) found for Pd−P distances in palladium bis(diphenylphosphino)ethane complexes.[12]

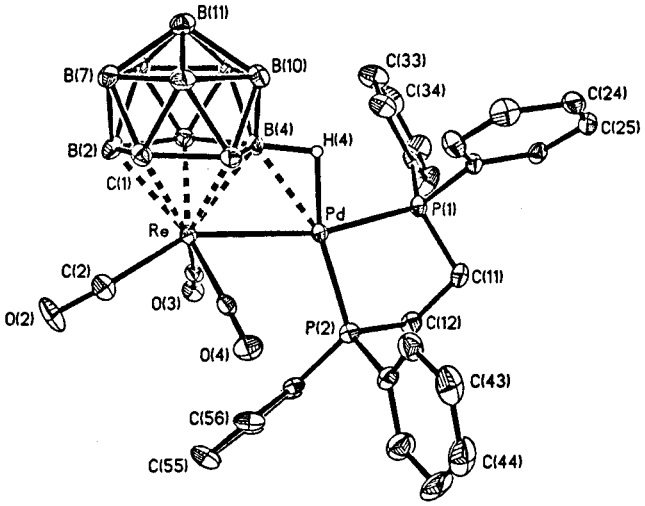

Figure 4. Structure of $[RePd(CO)_3\{Ph_2P(CH_2)_2PPh_2\}(\eta^5\text{-}7\text{-}CB_{10}H_{11})]$ (**5a**), showing the crystallographic labeling scheme. Thermal ellipsoids are shown at the 40% probability level. Only the agostic hydrogen atom is shown for clarity.

The IR spectrum of complex **5a** is almost identical with those of the RePt complexes **4**, with ν_{max}(CO) absorption bands at 2024 (vs), 1956 (m), and 1926 (s) cm^{-1} (Table 1). The room-temperature ^1H NMR spectrum (Table 2) is basic with a resonance at δ 2.25 for the cage CH proton, as is the $^{13}C\{^1H\}$ NMR spectrum at this temperature which displays two signals for the ReCO carbon nuclei (δ 196.9 and 194.0) with a peak integral ratio of 1:2. The latter information implies that a mirror plane exists in the molecule in solution that includes both of the metal atoms, the phosphorus atoms, and the cage carbon. This notion is further supported by the observation in the $^{11}B\{^1H\}$ NMR spectrum (Table 3) measured at room temperature of a set of four signals (2:4:2:2). The $^{31}P\{^1H\}$ NMR spectrum is also informative with the phosphorus nuclei appearing inequivalent (δ 62.9, 61.0, J(AB) 23 Hz), as expected. These results are at odds with both the above-described structural analysis of **5a** and the nature of compounds **4**, which were shown by X-ray and spectroscopic techniques to be asymmetric. Despite solubility difficulties, NMR measurements were made on **5a** at −90 °C. The ^1H NMR spectrum at this temperature revealed a broad peak at δ −5.03, typical of an agostic B−*H*⇀M proton,[10] while the $^{31}P\{^1H\}$ NMR spectrum displayed a pair of signals (δ 65.8, 65.6, J(AB) 20 Hz) which merely showed an enhanced second-order roofing compared with the spectrum obtained at ambient temperatures. Unfortunately, a sensible $^{11}B\{^1H\}$ NMR spectrum of **5a** could

(12) Allen, F. H.; Brammer, L.; Kennard, O.; Orpen, A. G.; Taylor, R.; Watson, D. G. *J. Chem. Soc., Dalton Trans.* **1989**, S1.
(13) (a) Henley, T. J.; Wilson, S. R.; Shapley, J. R. *Inorg. Chem.* **1988**, *27*, 2551. (b) Baker, R. T.; Calabrese, J. C.; Glassman, T. E. *Organometallics* **1988**, *7*, 1889.

Table 6. Selected Internuclear Distances (Å) and Angles (deg) for $[RePd(CO)_3\{Ph_2P(CH_2)_2PPh_2\}(\eta^5\text{-}7\text{-}CB_{10}H_{11})]$ (5a) with ESD's in Parentheses

Re−C(3)	1.944(4)	Re−C(4)	1.947(4)	Re−C(2)	1.954(4)	Re−B(4)	2.272(4)
Re−C(1)	2.314(3)	Re−B(2)	2.317(4)	Re−B(5)	2.335(4)	Re−B(3)	2.358(4)
Re−Pd	2.7858(4)	Pd−P(1)	2.2673(9)	Pd−P(2)	2.2738(10)	Pd−B(4)	2.333(4)
Pd−H(4)	1.74(4)	C(2)−O(2)	1.143(4)	C(3)−O(3)	1.152(4)	C(4)−O(4)	1.155(4)

C(3)−Re−C(4)	102.1(2)	C(3)−Re−C(2)	83.8(2)	C(4)−Re−C(2)	84.6(2)
C(3)−Re−Pd	74.04(10)	C(4)−Re−Pd	77.01(10)	C(2)−Re−Pd	147.27(12)
B(4)−Re−Pd	53.78(11)	C(1)−Re−Pd	121.14(8)	B(2)−Re−Pd	127.59(11)
B(5)−Re−Pd	79.37(10)	B(3)−Re−Pd	84.63(10)	P(1)−Pd−P(2)	85.22(4)
P(1)−Pd−B(4)	114.23(10)	P(2)−Pd−B(4)	160.46(10)	P(1)−Pd−Re	165.99(3)
P(2)−Pd−Re	108.78(3)	B(4)−Pd−Re	51.79(10)	B(9)−B(4)−Pd	146.0(3)
B(5)−B(4)−Pd	104.4(2)	B(3)−B(4)−Pd	113.5(2)	Re−B(4)−Pd	74.43(13)
O(2)−C(2)−Re	176.6(4)	O(3)−C(3)−Re	173.5(3)	O(4)−C(4)−Re	174.6(3)

Scheme 2. Rapid Isomerization Process at Ambient Temperatures in Complex 5a

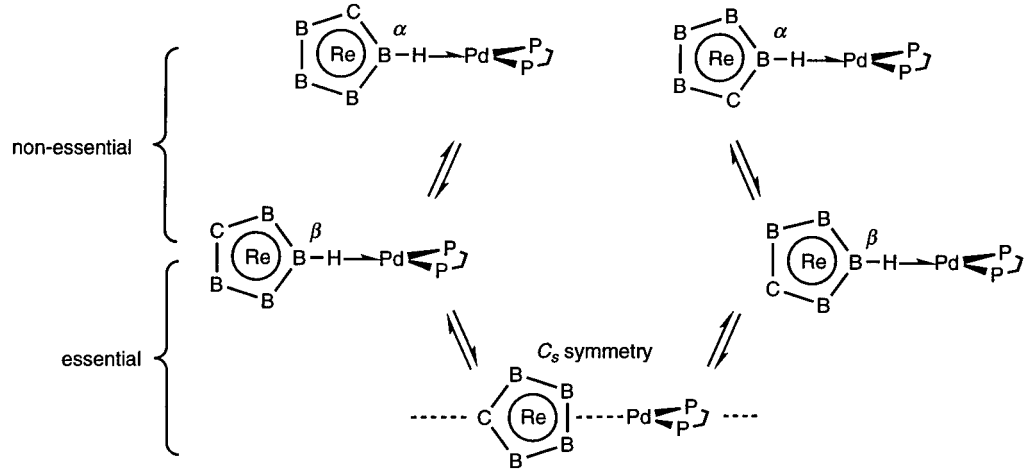

not be obtained at depressed temperatures. These results suggest that the low-temperature limiting species in solution probably corresponds to the solid-state structure with a B_β−H⇀Pd agostic bond. At ambient temperatures, a rapid isomerization process must be occurring in solution (Scheme 2). It is postulated that an exchange between both possible B_β−H⇀Pd-bonded systems is taking place considerably faster than the NMR time scale. This would be sufficient to generate local mirror symmetry at the cage by virtue of a transitional structure with C_s symmetry which lies between the two alternative B_β−H⇀Pd-bonded isomers. Thus, the room-temperature $^{13}C\{^1H\}$ and $^{11}B\{^1H\}$ NMR spectra are accounted for. Although inclusion of B_α−H⇀Pd-bonded moieties in this process cannot be ruled out, they are not necessary to achieve the desired effect. However, since the phosphorus nuclei remain inequivalent at room temperature, this fluxionality does not extend to complete mobility of the $Pd\{Ph_2P(CH_2)_2PPh_2\}$ fragment about the cage surface using multiple B−H⇀Pd bonds, as observed with the $Rh(PPh_3)_2$ unit in solutions of the complex [*exo*-5,10-$\{Rh(PPh_3)_2\}$-5,10-μ-$(H)_2$-10-*endo*-Au(PPh_3)-*nido*-7,8-Me_2-7,8-$C_2B_9H_9$].[14] High-temperature $^{31}P\{^1H\}$ NMR measurements up to 120 °C of DMSO-d_6 (DMSO = dimethyl sulfoxide) solutions of **5a** did not show any collapsing of the signals, so such fluxionality could not be thermally induced. Exchange of the $B_{\alpha/\beta}$−H bonds that form agostic linkages in molecules that contain the dicarbollide η^5-7,8-R_2-7,8-$C_2B_9H_9$ (R = H, Me) have been previously recorded.[15] In particular, the complex [WIr(μ-CC_6H_4Me-4)$(CO)_2(PPh_3)_2(\eta^5$-7,8-Me_2-7,8-$C_2B_9H_9)$] undergoes exchange between $B_{\alpha/\beta}$−H⇀Ir-bonded molecules in solution, slow enough on the NMR time scale to be able to detect the separate isomers.[15a]

The apparent dynamic behavior of the B−H⇀Pd system of **5a** in solution suggested that this complex may be a candidate for reaction with 2 e^- donor ligands, possibly leading to simple addition to the complex or even substitution of a CO ligand; the labilizing of Re−CO ligands in rhenium−platinum complexes has been documented.[9a] Treatment of CH_2Cl_2 solutions of complex **5a** with CNR (R = Bu^t, $C_6H_3Me_2$-2,6) at −78 °C yielded the complexes $[RePd(CO)_2(CNR)\{Ph_2P(CH_2)_2PPh_2\}(\eta^5\text{-}7\text{-}CB_{10}H_{11})]$ (R = Bu^t (**5b**), R = $C_6H_3Me_2$-2,6 (**5c**)). The reaction of **5a** with $CNBu^t$ consistently produced a second orange product, which, as yet, has not been identified. An incomplete X-ray diffraction study (due to poor quality crystals) of **5c** revealed that the Re atom was ligated by the $CNC_6H_3Me_2$-2,6 ligand and two CO groups and that the chelating $Ph_2P(CH_2)_2PPh_2$ ligand has maintained its bite on the Pd atom.

The IR spectrum of **5b** displayed a broad ν_{max}(NC) absorption at 2149 (m) cm^{-1} with two ν_{max}(CO) bands at 1955 (m) and 1898 (s) cm^{-1}. The ν_{max}(NC) absorption lies within the range expected for terminal CNR ligands (2080−2221 cm^{-1}).[16] The ^1H NMR spectrum of **5b** (Table 2) reveals the presence of the Bu^t group with a peak at δ 1.36 integrating to nine protons. The $^{13}C\{^1H\}$ NMR spectrum showed the two inequivalent CO

(14) Jeffery, J. C.; Jelliss, P. A.; Stone, F. G. A. *J. Chem. Soc., Dalton Trans.* **1993**, 1073.

(15) (a) Jeffery, J. C.; Ruiz, M. A.; Sherwood, P.; Stone, F. G. A. *J. Chem. Soc., Dalton Trans.* **1989**, 1845. (b) Hendershot, S. L.; Jeffery, J. C.; Jelliss, P. A.; Mullica, D. F.; Sappenfield, E. L.; Stone, F. G. A. *Inorg. Chem.* **1996**, *35*, 6561.

Scheme 3. Probable Pathway for Formation of Complexes 5b,c

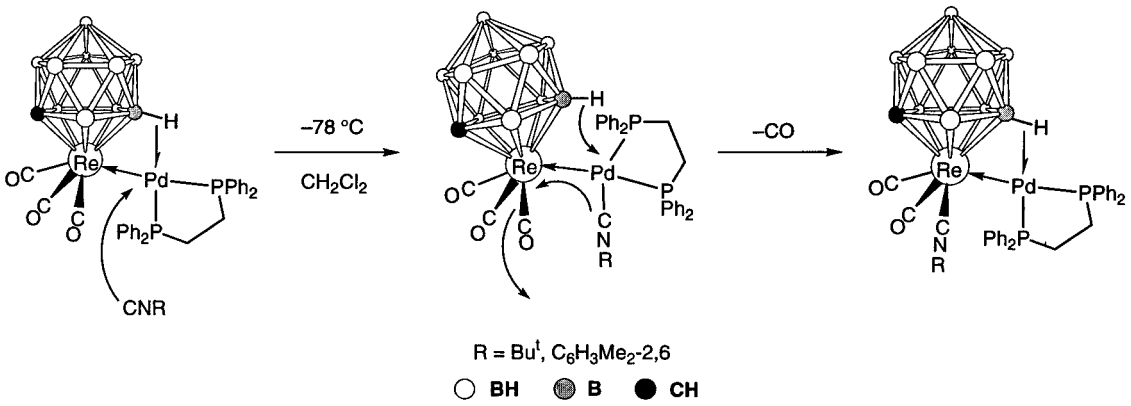

carbon nuclei with resonances at δ 197.9 and 197.8. In addition, there is a peak at δ 178.8 due to the *C*NBu^t nucleus. This latter signal may be compared with the corresponding signal for a terminal isocyanide ligand at δ 156.7 in the $^{13}C\{^1H\}$ NMR spectrum of the complex $[PdBr(CF{=}CF_2)(CNC_6H_3Me_2\text{-}2,6)_2]$.[17] The $^{11}B\{^1H\}$ NMR spectrum of **5b** (Table 3) comprised a set of six peaks (1:1:1:3:2:2), which implies there is a lack of symmetry in the complex. However, this is not due to the presence of a permanently fixed B−H⇀Pd agostic bond because, as with the parent complex **5a**, there was no evidence in the ^1H and $^{11}B\{^1H\}$ NMR spectra of **5b** for such a system in solution at ambient temperatures. It is likely, therefore, that the disposition of the CNBu^t ligand on the Re atom is causing the observed asymmetry by lying in a position cis to the Pd{$Ph_2P(CH_2)_2PPh_2$} group. The inequivalent phosphorus nuclei are observed, as expected, in the $^{31}P\{^1H\}$ NMR spectrum with doublet signals at δ 58.2 and 50.5 (J(PP) 35 Hz). The ^1H NMR spectrum of **5b** measured at −70 °C did reveal a broad signal at δ −4.91, which must correspond to a B−*H*⇀Pd proton. Presumably, this system involves a B_β−H bond in the ligating $\overline{CBBBB}$ face of the cage, although this can only be verified by an X-ray structure determination. Unfortunately, tractable crystals of **5b** could not be grown. Thus, complex **5b** seems to behave in a manner similar to **5a** in CH_2Cl_2 solutions, undergoing an exchange between B−H⇀Pd-bonded species at 25 °C while forming a static system at low temperature. Despite the very low solubility of complex **5c** in common solvents, the NMR spectra and partial X-ray analysis indicate that it is structurally very similar to **5b**. In particular, the 2,6-xylyl methyl groups appear as inequivalent singlets in the ^1H (δ 2.79 and 2.82) and $^{13}C\{^1H\}$ (δ 19.0 and 18.9) NMR spectra, due, as one might expect in this sterically crowded molecule, to hindered rotation about the Re−C−N−C^1(aryl) system.

The mechanism of formation of the complexes **5b**,**c** likely proceeds via initial attack of the isocyanide molecule at the palladium center of **5a**, a reaction that would be facilitated by lifting the agostic B−H bond from the Pd atom. The complexes **5b**,**c** would then be formed by migration of the CNR ligand, concomitant loss of CO, and reformation of the B−H⇀Pd linkage (Scheme 3).

Conclusions

A fresh vista has opened up in the field of rhenacarborane chemistry with the syntheses of the new Re−Pt and Re−Pd complexes **4** and **5** containing a monocarbon−carborane ligand, and further rhenium-metal bond-forming reactions employing the salts **2** are currently being investigated. The reactions of **5a** with isocyanide ligands indicate that the new binuclear metal complexes are themselves reactive precursors, and further studies with both the Re−Pt and Re−Pd compounds are in progress.

Experimental Section

General Considerations. All experiments were conducted under an atmosphere of dry nitrogen using Schlenk tube techniques. Solvents were freshly distilled under nitrogen from appropriate drying agents before use. Light petroleum refers to that fraction of boiling point 40−60 °C. Celite pads for filtration were ca. 4 cm thick. Chromatography columns (ca. 60 cm long and 1 cm in diameter) were packed with silica gel (Acros, 60−200 mesh). The NMR measurements were recorded at the following frequencies: ^1H at 360.13 MHz, ^{13}C at 90.56 MHz, ^{11}B at 115.55 MHz, and ^{31}P at 145.78 MHz. The reagents *nido*-7-NMe_3-7-$CB_{10}H_{12}$[18] and $[ReBr(CO)_5]$,[19] were made as previously described. The platina- and palladaphosphine complexes $[PtCl_2(PR_3)_2]$ (R = Ph, Et) and $[MCl_2\{Ph_2P(CH_2)_2PPh_2\}]$ (M = Pt, Pd) were synthesized by adding the appropriate phosphine to CH_2Cl_2 solutions of $[MCl_2(NCPh)_2]$ (M = Pt, Pd).[20] The materials $[N(PPh_3)_2]Cl$, $[NEt_3(CH_2Ph)]Cl$, I_2, and $TlPF_6$ were used as purchased from Aldrich.

Synthesis of the Salt $[N(PPh_3)_2]_2[Re(CO)_3(\eta^5\text{-}7\text{-}CB_{10}H_{11})]$. The carborane compound *nido*-7-NMe_3-7-$CB_{10}H_{12}$ (2.83 g, 14.79 mmol) was placed in a Schlenk tube and heated in vacuo at 80 °C for 24 h to remove traces of water. Naphthalene (ca. 2 mg) was added followed by THF (30 mL), which had been distilled from potassium−benzophenone and then stored over a potassium mirror. To this solution was added a single sodium lump (ca. 0.2 mL^3), and the mixture was refluxed for ca. 3 days. The salt $[Na]_3[nido\text{-}7\text{-}CB_{10}H_{11}]$ forms as an insoluble white adduct with THF, the formation time being variable (1−3 days). Approximately 12 h before the $[Na]_3[nido\text{-}7\text{-}CB_{10}H_{11}]$ is ready to use, the compound $[ReBr(CO)_5]$ (5.00 g, 12.31 mmol) is heated to reflux in dry THF (30 mL) in a reflux-Schlenk tube to convert it to $[ReBr(THF)_2(CO)_3]$.[21] When ready, the heating mantles are simultaneously removed from

(16) Dixon, K. R.; Dixon, A. C. In *Comprehensive Organometallic Chemistry II*; Abel, E. W., Stone, F. G. A., Wilkinson, G., Eds.; Elsevier Science Ltd.: Oxford, 1995; Vol. 9, Section 4.3.

(17) Christofides, A. *J. Organomet. Chem.* **1983**, *259*, 355.

(18) Plešek, J.; Jelínek, T.; Drdáková, E.; Heřmánek, S.; Štíbr, B. *Collect. Czech. Chem. Commun.* **1984**, *49*, 1559.

(19) Schmidt, S. P.; Trogler, W. C.; Basolo, F. *Inorg. Synth.* **1990**, *28*, 162.

(20) Anderson, G. K.; Lin, M. *Inorg. Synth.* **1990**, *28*, 60.

(21) Vitali, D.; Calderazzo, F. *Gazz. Chim. Ital.* **1972**, *102*, 587.

Table 7. Data for X-ray Crystal Structure Analyses

	2b	4a	5a
cryst dimens (mm)	0.20 × 0.22 × 0.42	0.25 × 0.25 × 0.25	0.14 × 0.25 × 0.50
formula	$C_{30}H_{55}B_{10}N_2O_3Re$	$C_{40}H_{41}B_{10}O_3P_2PtRe$	$C_{30}H_{35}B_{10}O_3P_2PdRe$
M_r	786.06	1121.06	906.22
cryst color, shape	pale yellow, prism	yellow, cube	orange, plate
cryst syst	orthorhombic	monoclinic	orthorhombic
space group	$Pna2_1$	$C2/c$	$P2_12_12_1$
T (K)	173	173	173
a (Å)	14.8741(13)	23.461(3)	11.7860(11)
b (Å)	16.749(3)	12.101(2)	12.7521(14)
c (Å)	14.632(2)	31.004(5)	23.640(3)
β (deg)		109.243(12)	
V (Å^3)	3645.3(7)	8310(2)	3553.0(7)
Z	4	8	4
d_{calcd} (g cm^{-3})	1.432	1.792	1.694
μ(Mo Kα) (mm^{-1})	3.367	6.389	4.032
F(000) (e)	1592	4304	1760
2θ range (deg)	2.7−55.0	2.7−55.0	3.4−55.0
data frame collcn time (per frame/s, overall/h)	10, ca. 6	20, ca. 10	10, ca. 6
no. of rflns measd	21 706	26 120	22 227
no. of indep rflns	7874	9464	8091
refinement method	full-matrix least-squares on all F^2 data	full-matrix least-squares on all F^2 data	full-matrix least-squares on all F^2 data
Flack parameter	0.017(5)		−0.007(3)
final residuals	$wR_2 = 0.034^a$ ($R_1 = 0.018$)^b	$wR_2 = 0.040^a$ ($R_1 = 0.021$)^b	$wR_2 = 0.040^a$ ($R_1 = 0.022$)^b
weighting factors	$a = 0.0064$; $b = 0.0^a$	$a = 0.0141$; $b = 0.0^a$	$a = 0.013$; $b = 0.0^a$
goodness of fit on F^2	0.842	0.989	0.981
final electron density diff features (max/min) (e Å^{-3})	0.45, −0.48	0.73, −0.57	0.79, −0.57

[a] Structure was refined on F_o^2 using all data: $wR_2 = [\sum[w(F_o^2 - F_c^2)^2]/\sum w(F_o^2)^2]^{1/2}$, where $w^{-1} = [\sigma^2(F_o^2) + (aP)^2 + bP]$ and $P = [\max(F_o^2,0) + 2F_c^2]/3$. [b] The value in parentheses is given for comparison with refinements based on F_o with a typical threshold of $F_o > 4\sigma(F_o)$ and $R_1 = \sum||F_o| - |F_c||/\sum|F_o|$ and $w^{-1} = [\sigma^2(F_o) + gF_o^2]$.

the two refluxing mixtures. The residual sodium lump is carefully removed from the $[Na]_3[nido\text{-}7\text{-}CB_{10}H_{11}]$ suspension using a spatula, which has been flame-dried in order to minimize intrusion of water into the mixture. Then the $[ReBr(THF)_2(CO)_3]$ solution, *while still hot* (ca. 60 °C), is transferred into the $[Na]_3[nido\text{-}7\text{-}CB_{10}H_{11}]$ suspension via a Teflon tube under pressure generated from the Schlenk N_2-vacuum line. The resulting mixture was stirred at room temperature for ca. 2 h. Following which, $[N(PPh_3)_2]Cl$ (14.13 g, 24.61 mmol) was added and stirring continued overnight. Solvent was removed in vacuo, and CH_2Cl_2 (50 mL) was added, followed by filtration through Celite. Solvent was reduced in volume in vacuo to ca. 30 mL, and the solution was refiltered through Celite. Crystallization from CH_2Cl_2−light petroleum (40 mL, 1:3) gave pale yellow microcrystals of $[N(PPh_3)_2]_2[Re(CO)_3(\eta^5\text{-}7\text{-}CB_{10}H_{11})]$ (**2a**) (16.50 g), which were dried in vacuo. The salt **2a** may sometimes be contaminated by up to 15% $[N(PPh_3)_2][nido\text{-}7\text{-}CB_{10}H_{13})]$. The presence of this salt does not inhibit the reactivity of **2a**, and it may be separated out by column chromatography during isolation of neutral products. The salt $[NEt_3(CH_2Ph)]_2[Re(CO)_3(\eta^5\text{-}7\text{-}CB_{10}H_{11})]$ (**2b**) was synthesized in exactly the same way using $[NEt_3(CH_2Ph)]Cl$ (5.61 g, 24.61 mmol) in place of $[N(PPh_3)_2]Cl$.

Synthesis of the Salt $[N(PPh_3)_2][ReI(CO)_3(\eta^5\text{-}7\text{-}CB_{10}H_{11})]$. The salt **2a** (1.31 g, 0.89 mmol) was dissolved in CH_2Cl_2 (30 mL) and cooled to −78 °C. A solution of I_2 (0.21 g, 0.81 mmol) in CH_2Cl_2 (15 mL) was added from a dropping funnel at a drop rate of ca. 1 drop s^{-1} to the cold solution of **2a**. Addition took ca. 3 h, after which time the reaction mixture was gradually warmed to room temperature and stirred for 1 h further. Solvent was removed in vacuo to leave an intensely colored yellow residue. This was redissolved in CH_2Cl_2 (10 mL) and chromatographed at −30 °C. Elution with neat CH_2Cl_2 removed an intense yellow band. Removal of solvent in vacuo yielded $[N(PPh_3)_2][ReI(CO)_3(\eta^5\text{-}7\text{-}CB_{10}H_{11})]$ (**3**) (0.75 g).

Syntheses of the Compounds $[RePt(CO)_3(L)_2(\eta^5\text{-}7\text{-}CB_{10}H_{11})]$ (L = PPh$_3$ or PEt$_3$, $(L)_2 = Ph_2P(CH_2)_2PPh_2$). (i) The compounds **2a** (0.20 g, 0.14 mmol), $[PtCl_2(PPh_3)_2]$ (0.11 g, 0.14 mmol), and $TlPF_6$ (0.10 g, 0.29 mmol) were placed together in a Schlenk tube which was then purged with N_2. To this was added THF (20 mL), and the mixture was stirred for ca. 2 h, after which time the IR spectrum of a sample from the reaction showed no further change. Solvent was removed in vacuo, and CH_2Cl_2 (25 mL) was added to the residue. Filtration through Celite gave a yellow solution, which was reduced in volume in vacuo to ca. 4 mL and chromatographed. Elution with CH_2Cl_2−light petroleum (2:1) removed a yellow fraction. Solvent was removed in vacuo, and crystallization from CH_2Cl_2−light petroleum (20 mL, 1:4) gave $[RePt(CO)_3(PPh_3)_2(\eta^5\text{-}7\text{-}CB_{10}H_{11})]$ (**4a**) (0.14 g). (ii) Using a similar procedure, the compounds **2a** (0.20 g, 0.14 mmol), $[PtCl_2(PEt_3)_2]$ (0.07 g, 0.14 mmol), and $TlPF_6$ (0.10 g, 0.29 mmol) yielded bright yellow microcrystals of $[RePt(CO)_3(PEt_3)_2(\eta^5\text{-}7\text{-}CB_{10}H_{11})]$ (**4b**) (0.10 g). (iii) A similar method using **2a** (0.69 g, 0.47 mmol), $[PtCl_2(Ph_2P(CH_2)_2PPh_2)]$ (0.31 g, 0.47 mmol), and $TlPF_6$ (0.50 g, 1.43 mmol) afforded yellow microcrystals of $[RePt(CO)_3\{Ph_2P(CH_2)_2PPh_2\}(\eta^5\text{-}7\text{-}CB_{10}H_{11})]$ (**4c**) (0.39 g) after crystallization from CH_2Cl_2−light petroleum (30 mL, 1:1).

Syntheses of the Compounds $[RePd(CO)_2(L)\{Ph_2P(CH_2)_2PPh_2\}(\eta^5\text{-}7\text{-}CB_{10}H_{11})]$ (L = CO, CNBu^t, $CNC_6H_3Me_2$-2,6). (i) Under similar conditions to those used for the preparation of **4c**, the reagent **2a** (0.14 g, 0.09 mmol), $[PdCl_2\{Ph_2P(CH_2)_2PPh_2\}]$ (0.05 g, 0.09 mmol), and $TlPF_6$ (0.10 g, 0.29 mmol) gave orange microcrystals of $[RePd(CO)_3\{Ph_2P(CH_2)_2PPh_2\}(\eta^5\text{-}7\text{-}CB_{10}H_{11})]$ (**5a**) (0.07 g) after chromatography, eluting with CH_2Cl_2−light petroleum (7:3), and crystallization from CH_2Cl_2−light petroleum (15 mL, 1:2). (ii) Complex **5a** (0.09 g, 0.10 mmol) was dissolved in CH_2Cl_2 (10 mL) and cooled to −78 °C. With stirring, CNBu^t (16 μL, 0.14 mmol) was added to this solution. The mixture was then warmed gradually to room temperature and stirred for 2 h further. Solvent was removed in vacuo, and CH_2Cl_2−light petroleum (4 mL, 3:1) was added to the residue. The solution was chromatographed, and elution with CH_2Cl_2−light petroleum (4:1) removed an orange fraction. Removal of solvent in vacuo and crystallization from CH_2Cl_2−light petroleum (10 mL, 1:4) yielded orange microcrystals of $[RePd(CO)_2(CNBu^t)\{Ph_2P(CH_2)_2PPh_2\}(\eta^5\text{-}7\text{-}CB_{10}H_{11})]$ (**5b**) (0.05 g). Con-

tinued elution with CH_2Cl_2−THF (50:1) removed a second orange fraction. Crystallization from CH_2Cl_2−Et_2O (5 mL, 1:4) gave orange microcrystals (0.01 g) of an, as yet, unidentified material. (iii) Using a similar procedure, complex **5a** (0.10 g, 0.11 mmol) and $CNC_6H_3Me_2$-2,6 (0.02 g, 0.15 mmol) yielded orange-brown microcrystals of $[RePd(CO)_2(CNC_6H_3Me_2\text{-}2,6)\{Ph_2P(CH_2)_2PPh_2\}(\eta^5\text{-}7\text{-}CB_{10}H_{11})]$ (**5c**) (0.08 g), which were crystallized from CH_2Cl_2−light petroleum (10 mL, 1:1).

Crystal Structure Determinations and Refinements. Crystals of **2b** were grown by diffusion of Et_2O into a CH_2Cl_2 solution of the salt, while those of **4a** and **5a** were grown by diffusion of light petroleum into CH_2Cl_2 solutions of the complexes. The crystals were mounted on glass fibers, and low-temperature data were collected on a Siemens SMART CCD area-detector three-circle diffractometer using Mo Kα X-radiation, $\bar{\lambda} = 0.710\ 73$ Å. For three settings of ϕ, narrow data frames were collected for 0.3° increments in ω. In all cases, a total of 1321 frames of data were collected, affording more than a hemisphere of data. It was confirmed that crystal decay had not taken place during the course of the data collections. The substantial redundancy in data allows empirical absorption corrections (SADABS[22]) to be applied using multiple measurements of equivalent reflections. The data frames were integrated using SAINT,[22] and the structures were solved by conventional direct methods. The structures were refined by full-matrix least-squares on all F^2 data using Siemens SHELXTL version 5.03,[22] with anisotropic thermal parameters for all non-hydrogen atoms. Cage carbon atoms were identified from the magnitudes of their anisotropic thermal parameters and from a comparison of the bond lengths to adjacent boron atoms. With the exception of the agostic B−*H*⇀M (M = Pt, Pd) protons, all hydrogen atoms were included in calculated positions and allowed to ride on the parent boron or carbon atoms with isotropic thermal parameters ($U_{iso} = 1.2\ U_{iso\ equiv}$ of the parent atom except for Me protons where $U_{iso} = 1.5\ U_{iso\ equiv}$). The agostic B−*H*⇀M hydrogen atoms in **4a** and **5a** were located in difference Fourier syntheses, and their positions and isotropic thermal parameters were refined. All calculations were carried out on Silicon Graphics Iris, Indigo, or Indy computers, and experimental data are recorded in Table 7.

(22) Siemens X-ray Instruments: Madison, WI, 1995.

Molecular Orbital Calculations. A semiempirical ZINDO molecular orbital calculation was carried out using INDO1 parameters with atomic coordinates taken from the X-ray crystal structure determination on **2b**. The EHMO calculations were based on conventional parameters.

Cyclic Voltammetry. Experiments were carried out using a BAS100B/W electrochemical workstation with a Pt disk working electrode (0.5 mm diameter) and a supporting electrolyte of 0.1 M $[NBu^n_4][PF_6]$. Measurements were made on 1 mM CH_2Cl_2 solutions of **2a** at a range of scan rates (200 mV s^{-1} to 100 V s^{-1}) both in the absence and presence of 1 mM $[Co(\eta^5\text{-}C_5H_5)_2]Cl$ to confirm the magnitude of the oxidation wave as a 1 e^- process. Potentials are measured relative to the $[Fe(\eta^5\text{-}C_5H_5)_2]^+/[Fe(\eta^5\text{-}C_5H_5)_2]$ redox pair.

Acknowledgment. We thank the Robert A. Welch Foundation for support (Grant No. AA-1201) and Dr. Stephen Gipson (Baylor University) for cyclic voltammetry measurements.

Supporting Information Available: Tables of complete atomic coordinates and *U* values, bond lengths and angles, and anisotropic thermal parameters and ORTEP diagrams for **2b**, **4a**, and **5a** (34 pages). Ordering information is given on any current masthead page.

OM9709143